13th World Conference on Earthquake Engineering
Vancouver, B.C., Canada
August 1-6, 2004
Paper No. 125

DISLOCATION AND STRONG GROUND MOTION ZONING UNDER SCENARIO FAULTS FOR LIFELINES

Shiro TAKADA[1], Yasuko KUWATA[2], Abbas MAHADAVIAN[3], Resa RASTI[4] and Tsutomu IMAI[5]

SUMMARY

Present paper proposes a seismic hazard map in Tehran City to evaluate the seismic safety of gas supply systems extended whole in the city. First, the seismo-tectonic feature in Tehran area is investigated and scenario active faults that cause severe earthquakes are specified giving fault parameters. Based on the fault analysis, synthetic strong ground motions are estimated on the surface ground by using convolution method for element earthquakes and non-linear amplification factors. Then surface fault dislocation is estimated by using elastic dislocation theory. Furthermore, the potential of liquefaction and land slide is involved in the hazard map.

INTRODUCTION

According to the zoning maps of seismic hazard prepared for Iran (Iran Code 2800), Teheran is located in a region with relatively high seismic hazard. Therefore, it is of special importance to identify the seismogenic factors of the region. Then, strong ground motion parameters were estimated along the gas pipeline and pressure release stations for making them resistant to earthquake.

Complementary seismotectonic studies were performed including the re-study of satellite images and aerial photographs on the near site area with a radius of 100 kilometers. In some cases, the faults near the new trenches of expressways and foundation excavations of the buildings under construction were inspected. Finally, the locations of faults in and around Teheran were exhibited on the map of Teheran. The seismotectonic profile of the near faults was prepared and their situations were determined. The city of Teheran is located in the boundary of the two seismotectonic provinces, i.e., Alborz and Central Iran. This boundary is not clear cut. On the other hand, the epicentral errors of the past earthquakes are more than tens of kilometers. Therefore, seismic data were collected in a radial way.

[1] Professor, Kobe University, Kobe, Japan. Email: takada@kobe-u.ac.jp
[2] Assistant professor, Kobe University, Kobe, Japan.
[3] Assistant professor, Power and Water Institute of Technology, Tehran, Iran.
[4] Lecturer, Power and Water Institute of Technology, Tehran, Iran.
[5] Engineer, Mitsubishi Heavy Industries, Ltd., Hiroshima, Japan

Strong ground motion and surface ground dislocation due to fault ruptures are estimated by introducing fault rupture analysis and elastic dislocation theory. Also, ground failure of liquefaction and land slide potential are estimated along the gas network and stations.

FAULTS AND STRONG GROUND MOTIONS

Major Faults and Parameters

Table 1 listed the major active faults near Tehran. As an example, outline of the North Tehran Fault and relevant historical earthquakes is shown below. The North Tehran Fault is 90 km long and located on the north of Teheran. It has E-W to ENE-WSW strike and has thrust mechanism. This fault has been traced in the North Tehran mountains from the east of Lashgarak (Saboo Village) in the northeast of Tehran to KazemAbad locality (2 km east of Kalak and north of Tehran-Karaj Expressway) and in the city of Karaj in the west. In most places including north of Tehran and at the foothills, this quaternary alluvia has caused the Eocene Karaj Formation (Alborz Border Folds) to be thrust over Hezardarreh and NTF (pediment zone of Central Iran). The sudden change in height between the city of Tehran (with an average elevation of 1300 masl) and its highest peak (Tochal, 3933 masl) in a distance of less than 10km is a significant topographic characteristic of Tehran for which North Tehran thrust movements are responsible (Tchalenko et al. [1]). The thrust dip of this fault is highly variable: 10-45 degrees towards north on the west of Kan, 27-40 degrees towards north on the east of Kan, 70-80 degrees towards NW at Farahzad, 40 degrees towards NNW on the west of Lashgarak Valley and about 30 degrees towards north on the NE of Saboo Village. It can be assumed anyway that the dip of NTF is milder than 75 degrees, because this fault

Table 1 Characteristics of some important faults at the project area

Fault names	Approximate. Length (Km)	Mechanism	General trend	Max attributed magnitude (M)
North Tehran	90	Thrust	E-W	7.3
Niyavaran	18	Thrust with left lateral strike-slip component	ENE-WSW	6.5
Mahmoodiyeh	11	Thrust	E-W	6.2
Davoodiyeh	4.5	Thrust	E-W	5.7
South Mehrabad	10	Thrust	NE-SW	6.2
North Ray	17	Thrust	E-W	6.5
South Ray	>18	Thrust	ENE-WSW	>6.5
Kahrizak	>40	Thrust	E-W	6.9
Parchin	73	Reverse	NW-SE	7.2
Qasr Feeroozeh	18	Reverse	NW-SE	6.5
Shiyan Kowsar	15	Thrust	NW-SE	6.4
Upper Telo	10	Thrust	NW-SE	6.2
Lower Telo	20	Thrust with right lateral strike-slip component	NW-SE	6.5
Latyan	11	Reverse	WNW-ESE	6.2
Baghfeyz	4.5	Thrust with right lateral strike-slip component	NW-SE	5.7
Sorkhesar	22	Thrust	E-W to WNW-ESE	6.6
Hamsin	9	Thrust	E-W to WNW-ESE	6.1
Bibishahrbanoo	5	Thrust	WNW-ESE	5.8

is a branch of Mosha Fault. Hence, a milder dip than that of Mosha Fault should be considered for it to reach Mosha Fault in depth.

This is a seismogenic quaternary alluvia considered as a branch of Mosha Fault. Contrary to Mosha Fault, this quaternary alluvia does not have a distinct fault scarp (Berberian and Yeats [2]). Due to the scarcity of data, its seismic history is not clearly known, but the following earthquakes have been probably caused by this fault (Berberian et al. [3]):

- The earthquake of Feb 23, 958 B.C., with an estimated Ms 7.7(ISC) and 7.4 (Ber)
- The earthquake of May 1177 between Shahr Ray and Qazvin, estimated Ms 7.2
- The earthquake of December 24, 1895, Tehran
- The epicenter of the earthquake of Roodbar Qasran, M4.1, has been determined 25 and 35 km north of North Tehran thrust in the north of the city of Tehran, and this earthquake has probably resulted from the movement of this fault, but there is no strong reason to support this idea.
- The earthquake of Najjarkola NE of Tehran, Oct 26, 1989

As for the earthquakes of 855-856 (exact date not known) and 1177, the responsible quaternary alluvia or faults cannot be determined, but could have caused the rupture of NTF.

After the close discussion about faults near Tehran, we could reach to following results with respect to earthquakes caused active faults. We use two approaches to estimate strong ground motion and acceleration at the seismic base: probabilistic and deterministic approaches. For the latter approach, we assumed 4 scenario earthquakes as shown in Table 2, which lists fault parameters to calculate strong ground motions. The sketch of scenario faults for both approaches is shown in Fig.1.

Table 2 Scenario faults in the project

Case	Fault	L (km)	W (km)	Small M	Moment M	D (m)	τ (sec)	Θ (°)	δ (°)	λ (°)	n	Upper depth of fault (km)
Case1	North Ray	17	9	5	6.5	0.63	1.57	277	75	90	5	5
Case2	South Ray	20	10	5	6.6	0.7	1.85	277	75	90	6	5
Case3	North Tehran	30	30	5.3	7.2	1.41	2.78	311	75	90	9	0
Case4	Mosha	20	22	5.3	7.1	1.25	2.03	309	75	90	8	0

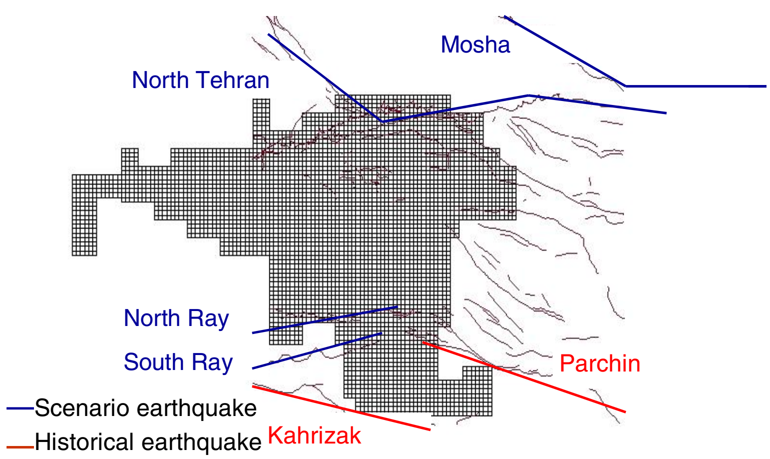

Fig. 1 Faults for scenario earthquake

Statistical Ground Motions

In the probabilistic approach, peak ground acceleration is calculated based on the statistical analysis of available earthquake catalogue entries for a certain return period. In this method, at first the probabilistic event of earthquake with magnitude M at distance R is calculated. The seismic hazard will be obtained based on area and line source with random variable under the Poisson process. Under the assumption of the Poisson process, the earthquake occurrence probability during the period ΔT, in which the intensity Y is over y, is given by;

$$P(\nu;\Delta T) = 1 - \exp(-p(Y \geq y)\cdot \Delta T) \tag{1}$$

Fig. 2 shows the exceedance probability of ground motion for return periods. Table 3 lists the fault parameters for statistical ground motions. Fig. 3 shows the procedure to simulate earthquake ground motion. First, a time history of ground motion is simulated for a given fault and then an enveloped velocity response spectrum is determined in order to cover relevant velocity response spectra. Finally, a sample time history for the statistical ground motions is obtained.

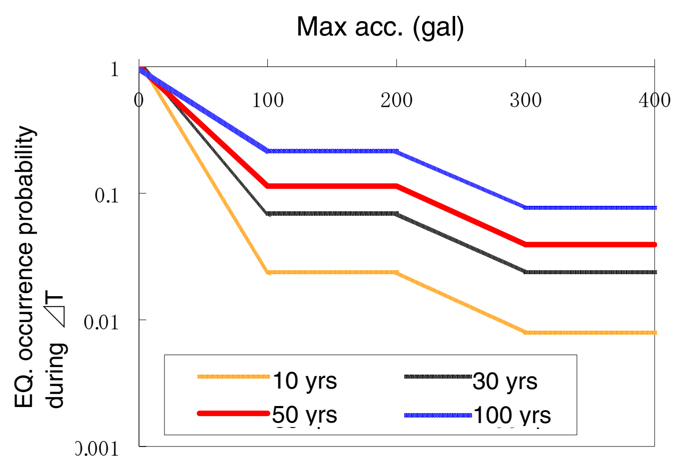

Fig. 2 Earthquake occurrence probability for given return periods

Table 3 Fault parameters for statistical ground motions

Case	Fault	L (km)	W (km)	Small M	Moment M	D (m)	τ (sec)	θ (°)	δ (°)	λ (°)	n	Upper depth of fault(km)
Case8	Parchin	73	28	5.3	7.2	1.41	6.76	250	75	0	9	5
Case9	Parchin	73	28	5.3	7.2	1.41	6.76	250	75	90	9	5
Case10	Parchin	73	28	5.3	7.2	1.41	6.76	250	75	180	9	5
Case11	Parchin	73	28	5.3	7.2	1.41	6.76	250	75	270	9	5
Case12	Kahrizak	50	20	5.2	6.9	0.99	4.63	260	75	0	7	5
Case13	Kahrizak	50	20	5.2	6.9	0.99	4.63	260	75	90	7	5
Case14	Kahrizak	50	20	5.2	6.9	0.99	4.63	260	75	180	7	5
Case15	Kahrizak	50	20	5.2	6.9	0.99	4.63	260	75	270	7	5

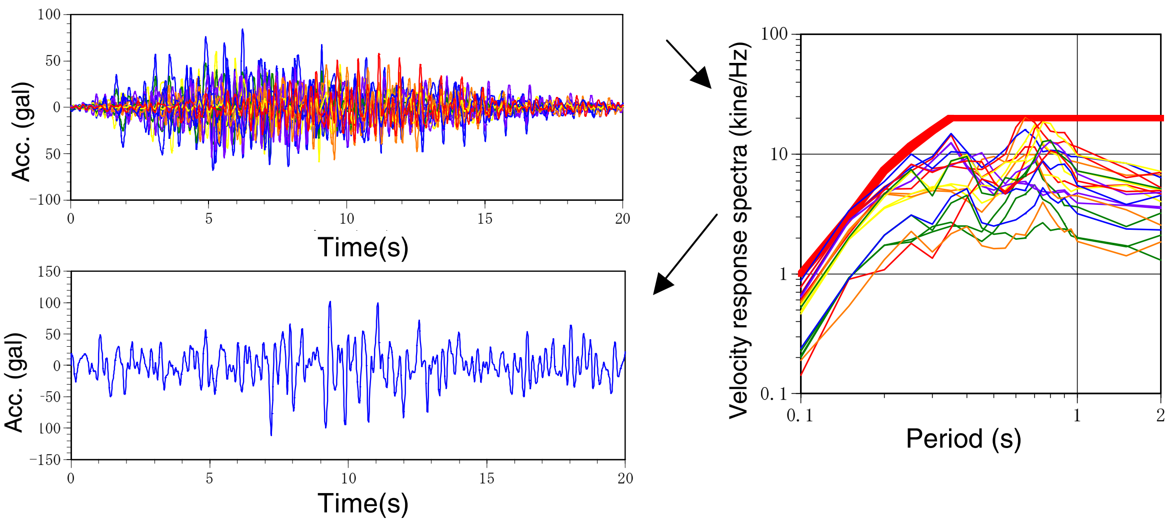

Fig. 3 Spectra compatible ground motions

Deterministic Ground Motions

This is based on the way that we choose the scenario fault that may cause damage and a hypothesis based on the most significant damage scenario that is considered as basic and indispensable approach to assess the earthquake resistance of the gas network. In this method the target area may be meshed by 500x500 m. and time-histories of seismic base motion are generated for each mesh. For such assessment, Geographic Information System (GIS) is very powerful tool with visible appearance. This project also used it.

For calculating the bedrock motion we have used synthetic wave method by using a computer program. This program is written by Takada et al [4], [5]. For generating a wave associated with small quakes, the Boore's statistical simulation method [6] is used. Following the spectrum model of the source fault, different initial random numbers are applied to the spectrum to generate the waveform of small quakes. A regional wave attenuation value and empirical screening of the duration time are used in the calculation. In this empirical wave synthetic method, it is not necessary to evaluate the characteristics of wave propagation route and the ground. Although the advantageous features of the empirical Green Function are not fully taken, the rupture propagation on the fault surface and the geometrical relation between the fault and any arbitrary point are well considered in the computation. For generating a synthetic wave, the Fourier Spectrum of acceleration induced by a fault rupture is calculated from summation of spectra due to small earthquake as shown in Fig. 4.

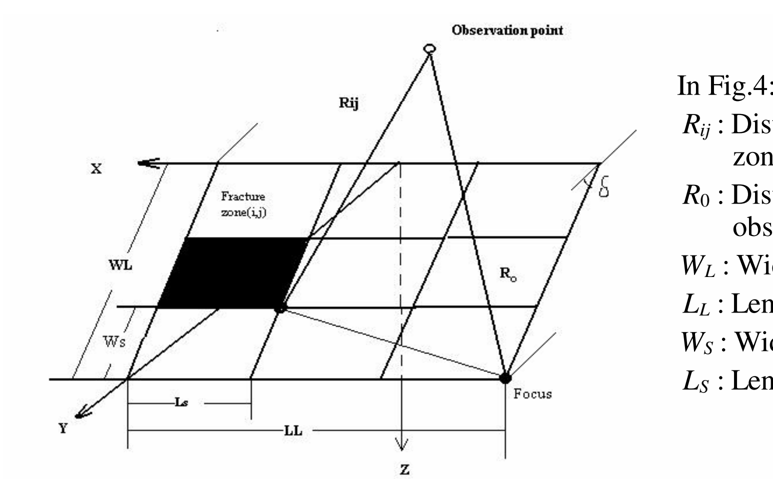

In Fig.4:

R_{ij} : Distance from the rapture starting point of zone (i, j) to observed point on ground

R_0 : Distance from focus of a large earthquake to observed point on ground

W_L : Width of fractured zone of a large earthquake

L_L : Length of fractured zone of a large earthquake

W_S : Width of small fractured zone

L_S : Length of small fractured zone

Fig. 4 Fault model for synthetic wave generation [7]

Therefore, we can write:

$$A_L(f) = \sum_{i=1}^{n_L} \sum_{j=1}^{n_w} A_S(f) \exp(-if \cdot t_{ij}) + \sum_{i=1}^{n_L} \sum_{j=1}^{n_w} \sum_{k=1}^{(n_d-1)n'} A_S(f) \exp(-if \cdot t_{ijk}) \qquad (2)$$

where, $A_L(f)$: Fourier Spectrum of acceleration (due to rupture of whole fractured zone in the fault)
$A_S(f)$: Fourier Spectrum of acceleration for small fractured zone

In Eq. (2) the first term in the right side gives the effect of time delay (attenuation) between the focus of large quake (start point of the fractured zone of the fault) and the focus of small quake (start point of a zone (i, j)), while the second term is the effect of time delay between the start and end points of the zone (i, j) (attenuation during the fracture time in a small quake).

The other parameters are as follows:

- t_{ij}: time delay between focus of large earthquake and small quake due to zone (i, j)
- t_{ijk}: time delay due to the fracture propagation in zone (i, j)
- n_L: number of zones along the length of fractured part of the fault
- n_W: number of zones along the width of fractured part of the fault
- n_d: ratio of the time delay in length direction to the one in the width direction
- n': adjusted coefficient for demolishing the apparent period due to the fractions of fractured time of a small zone.

The details to determine other fault parameters to obtain the time histories are referred to our paper. Fig.5 shows the result of accelerogram for predicted ground motion as an example of the North Ray earthquake. Figs. 6 and 7 show the distribution of base rock and surface accelerations for a scenario earthquake.

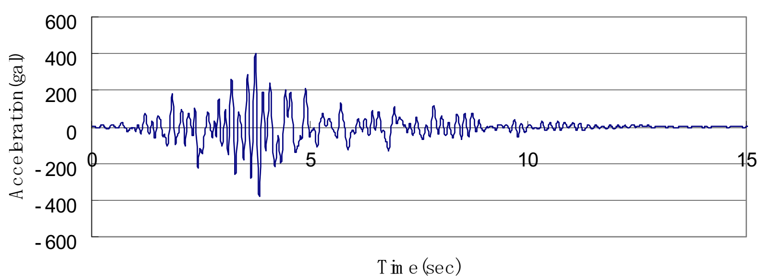

Fig. 6 Base rock acceleration for the North Ray earthquake

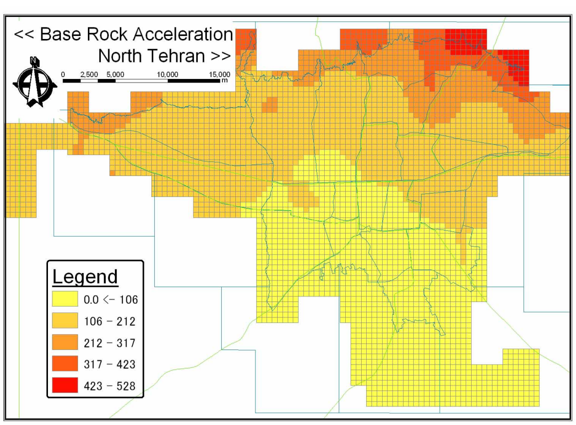

Fig.7 Base rock acceleration of North Tehran EQ

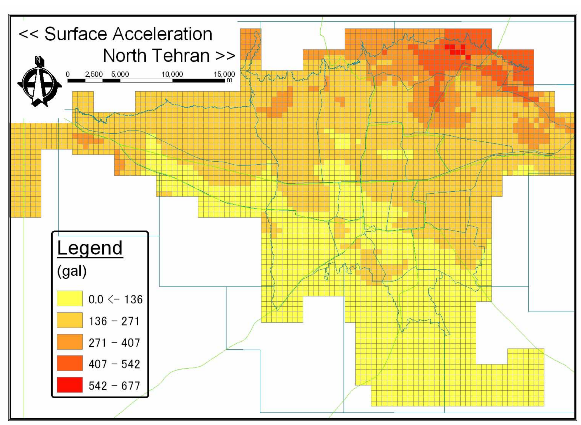

Fig.8 Surface acceleration of North Tehran EQ

SURFACE FAULT DISLOCATION

From mechanical point of view, a fault is a phenomenon in which both sides of an underground discontinuity slide relative to each other. From seismological point of view the motion process is of particular importance and it is not uncommon to call what is in fact fault motion, simply a fault. A discontinuity of displacements is called slip, and the surface causing it (fault slip) is thought to be rectangular. However a discontinuity of a rectangular shape is difficult to deal with by the general theory of elasticity. One way to bridge this difficulty is to use a discontinuity theory.

Steketee [8] applied the well known from material science and crystal structures discontinuity concepts to earthquake faults and called the large discontinuities (compared to those in crystals etc.) caused by faults dislocations. In this research we apply his "elastic dislocation theory" to earthquake induced ground displacements, propose analysis equations and perform simulations using the magnitude of fault displacement as a parameter. In this section we explain the elastic dislocation theory, and introduce the equations of Okada [9] which are derived from the equations of Steketee [8], Press [10] for a real fault model. Although the dislocation theory is simply an extension to the treatment of a continuous body subjected to discontinuities, in order to numerically introduce the earthquake motion, we first rewrite the governing partial differential equations under the assumptions of small strain and linear elastic stress-strain relation. First, we adopt a 3-D Cartesian coordinate system, and introduce the equation of motion of an infinitesimal cube in tensor notation. While, the stress-strain relation in the loading and unloading process is governed by the Hook's law. We could obtain the equation of motion of the continuous body by substituting the stress-strain relation into the equation of motion of an infinitesimal cube. In case of isotropic coordinate system, we arrive at the following equation,

$$(\lambda+\mu)u_{ji.j}+\mu u_{i,jj}+f_i-\rho\ddot{u}_i=0 \tag{3}$$

The above second order partial differential equation can be rewritten as an integral equation provided an integration mesh of size L is adopted (Betti's theorem).

When a force is applied along the position vector ξ at its source point (force application point), i.e. when the force is acting at the current time along direction *n*, the displacement vector along the component direction *i* of the position vector *x* can be expressed in terms of the Green's function $G_{in}(x;\xi)$. In this way, the physical properties of the elastic body like density, elastic modulus, and the fault movement boundary conditions can be expressed as functions in space. The Green's function $G_{in}(x;\xi)$ related to Eq. (3) has to satisfy the following special differential equation. By applying equation for two different equilibrium states, which are solutions of the governing equations, to the Betty's theorem, we get,

$$u_n(x,t)=\iiint_V f_i(\xi,\tau)G_{ni}(x;\xi)dV(\xi)+\iint_S\left\{T_i(u(\xi),n)G_{ni}(x;\xi)-u_i(\xi)c_{ijkl}(\xi)n_j\frac{\partial G_{nk}(x;\xi)}{\partial\xi_l}\right\}dS(\xi) \tag{4}$$

This equation gives the displacement at point *x* along direction *n* when a force is applied at the source point ξ along direction *i*.

Here, we further derive equations based on the dislocation model and assuming fault movement as boundary condition, and the derived in linear elastic equations.

$$[u(\varsigma)]=u^+(\xi)-u^-(\xi) \tag{5}$$

The boundary conditions can be expressed as follows,

$$T(u,n^{+})+T(u,n^{-})=0 \tag{6}$$

If we apply Eq.(4) for the outer side of the domain V constrained by the fault boundary, we can get the final closed form to calculate surface fault dislocation near the fault line. Fig. 9 shows the distribution of fault displacement of the North Tehran earthquake as an example of simulation.

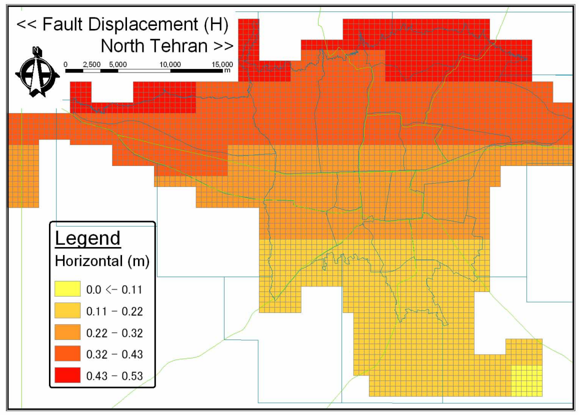

Fig.9 Horizontal fault displacement of North Tehran earthquake

LIQUEFACTION AND LAND SLIDE

Liquefaction Potential

Tehran is not located near the sea, but there is possibility for liquefaction those areas with sandy soil and low level of water table. Our study is based on "manual for Zonation on Seismic Geotechnical Hazards" by TC4, ISSMFE (1993) and "Japanese Design Specification of Highway Bridge (2000)". Three ranks for liquefaction are as follows.

Rank I: Beach rivers, beach seas, old channel bed or riverbed, coastal area and reclaimed areas are with high potential liquefaction.

Rank II: Alluvium area sandy hills are with medium potential liquefaction.

Rank III: Mountain and high level area have no potential of liquefaction.

There are 3 grades for estimating liquefaction potential in the manual. A detailed analysis based on geological investigation results and numerical analyses is used. The following information on soil properties and seismic motion was available in the study: (1) borehole logs with results of Standard Penetration Tests (SPT), (2) soil type and layers, (3) physical properties of soil, and (4) peak ground acceleration. Considering the above, a combination of the liquefaction resistance factor (F_L) method and the liquefaction potential (P_L) method was used in the study. The results of liquefaction potential index (P_L), horizontal displacement (δ_h) and settlement are calculated. Following soil parameters are used for analyzing (Table 4).

Table 4 Soil parameters for analysis

Soil type	Depth of layer	Water table	Fc (%)	D_{50} (mm)	D_{10} (mm)	Unit weight (kN/m^3)
Gravel	20	5-20	5	5	0.1	21
Sand	20	5-20	15	2.5	-	20
Clay	No possibility of liquefaction					

As the result for liquefaction, a part of south area in Tehran is assessed as to have potential for liquefaction. Fig. 10 shows the PL value in the target area.

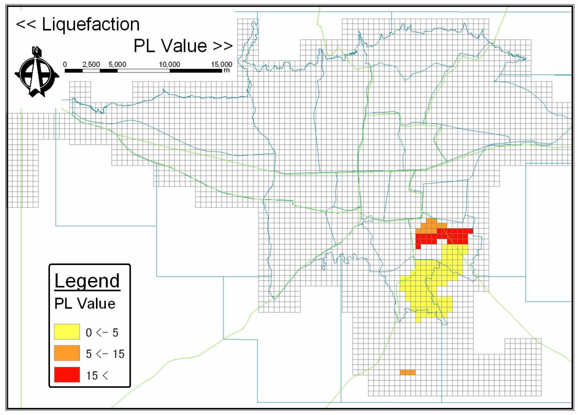

Fig.10 PL value

Landslide potential

Since Tehran is located on the slope of the Alborz Mountain, landslide is one of the possible hazards, especially in the north of Tehran. The up northern parts of the city, which are located near to the North Tehran Faults, and the hills of Abassabad near to the active faults are expected to have high potential for landslide. This can be extended for the areas located near Gisha and Vanak. In the south of Tehran, the landslide potential is not so high because of very gentle slope. One point to say in the north of Tehran is the quality of ground layers which have been very stable in the open-cuts, trenches or natural stability even in very sharp slopes.

A preliminary and rough estimation for the landslides potential in each mesh in Tehran is also given. Landslide potential is classified based on soil condition, V_S and N value, depth of seismological base rock, slope of base rock, slope of surface ground, acceleration and amplification of earthquake. It is worthy to note that if $V_S < 300$ m/s, $N_{spt} < 30$, slope of surface ground > 80%, acceleration > 400 gal and amplification of earthquake more than 1.5, it is evaluated as high potential landslide.

CONCLUSIND REMARKS

Present paper treats a seismic hazard map for the seismic safety evaluation for lifelines in Tehran area under statistical and deterministic earthquakes. Results are summarized as follows.

1. Seismotectonic features near Tehran area are investigated based on satellite image and aerial photographs, then major faults inducing significant ground motions are specified as scenario faults for the evaluation of lifeline seismic safety.
2. Statistical ground motions under a certain return period are calculated under consideration of past earthquakes occurred within 100 km near Tehran. Time histories of ground motions compatible to response spectra are obtained for fault parameters.
3. Deterministic ground motion is synthesized by employing the convolution method, which gives an element ground motions with smaller earthquake magnitude reflecting source mechanism and wave propagation pass.
4. Distributions of fault surface dislocation are obtained by applying the Green Functions based on the elastic dislocation theory.
5. Liquefaction and landslide potential are identified for 500m x 500m mesh areas in Tehran city.

ACKNOWLEDGMENT

This study was conducted by the Investigation Research Committee for Earthquake Resistance Evaluation of Tehran Gas Supply System headed by Professor Shiro Takada of Kobe University, as part of the "Research Project for Strengthening and Control of Tehran Gas Network Against Earthquake"(fiscal 2002 through 2003), commissioned by National Iranian Gas Company (NIGC) and Greater Tehran Gas Company (GTGC). We would like to express our gratitude to all related parties, including authorities, experts and staffs of NIGC and GTGC for their kind assistance in our study.

REFERENCES

1. Tchlenko, J.S., Berberian, M., Iranmanesh, H., Baily, M. and Arsovsky, M. "Tectonic framework of the Tehran region." Geol. Surv. Iran. Rep. 29, 1974: 7-46.
2. Berberian, M., and Yeats, R.S. "Patterns of Historical Earthquake Rupture in the Iranian Plateau," bull. Seism. Soc. Am. 1999: 89, 129-39.
3. Berberian, M., Qorashi, M., Arzhangravesh B., and Mohajer-Ashjai, A. "Recent tectonics, seismotectonics, and earthquake-fault hazard study of the Greater Tehran region (Contribution to the Seismotectonics of Iran, Part V)", Geol. Surv. Iran, Rep. 1985: 56, 316 (in Persian).
4. Takada, S., Fukuda, K. and Mori, K. "Estimating earthquake motion near fault in the light of asperity," Memoirs of Construction Engineering Research Institute 1998: 40-B, 23-39.
5. Takada, S., Hassani, N. and Fukuda, K. "Definition of fault near field based on seismic wave energy," (submitted to Journal of Earthquake Spectra), 2000.
6. Boore, D.M. "Stochastic simulation of high-frequency ground motions based on seismological models of the radiated spectra," Bull. Seism. Soc. Am. 1983: 73 (6), 1865-94.
7. Takada S., Hassani N., and Rasti R. "Scenario fault and micro-zonation in Tehran City," Memoirs of Construction Engineering Research Institute 2000: 42-B, 37-56.
8. Steketee, J. A. "On volterra's dislocations in a semi-infinite medium, Can. J. Phys. 1958: 36, 192-205,
9. Okada, Y. "Surface Deformation in a Half-space, Bull. Seism. Soc. Am. 1983: 1135-54.
10. Press, F. "Displacements, strains and tilts at teleseismic distances, J. Geophys. 1965: 70 (10), 2395-2412.
11. Jafari, M.K. and Asghari, A. "Seismic geotechnical microzonation of southwest of Tehran," Report of International Institute of Earthquake Engineering and Seismology of Iran 1998: 58-80.
12. Jafari, M.K., Pourazin, Kh. and Kamalian, M. "Seismic geotechnical microzonation of southeast of Tehran," Report of International Institute of Earthquake Engineering and Seismology of Iran 1999: 50-84.